

## MICROWAVE PROPERTIES OF LOW-TEMPERATURE CO-FIRED CERAMIC SYSTEMS\*

RICHARD G. GEYER<sup>a</sup>, LIANG CHAI<sup>b</sup>, AZIZ SHAIKH<sup>b</sup>, AND VERN STYGAR<sup>b</sup>

<sup>a</sup>National Institute of Standards and Technology  
RF Technology Division, M.S. 813.01  
Boulder, CO 80303

<sup>b</sup>Ferro Electronic Material Systems, 1395 Aspen Way, Vista, CA 92083

### ABSTRACT

Co-fired, patterned multilayer ceramic structures permit the design of compact, dense microwave circuits, components and devices spanning the frequency range from 800 MHz to 77 GHz. Critical parameters affecting the performance of these low-temperature co-fired ceramic (LTCC) systems are the dielectric properties of the co-fired ceramic and the metal loss occurring in the patterned circuit. These parameters have different dependences on frequency and temperature, and therefore their contributions to total insertion loss change as a function of application frequency and temperature. The contributions to microstrip attenuation loss of each of these critical parameters are analyzed at 10 GHz. Various dielectric resonator methods are used for accurate determinations of the substrate intrinsic dielectric properties and the metal surface resistance. These data were used to evaluate individual contributing factors of attenuation loss. The total computed attenuation loss compared well with that measured with a microstrip ring resonator. This characterization aids the optimal development of multilayer electronic circuits for the application frequency. It also provides the material scientist with the necessary focus on important dielectric, metallization, and fabrication processing issues encountered in the development of high-performance LTCC high-frequency application packages.

### INTRODUCTION

Continuing expansion of mobile communication systems and microwave links has lead to a dramatic increase in circuit fabrication technologies [1]. Most applications require high-volume, low-cost microelectronics packaging technologies, while maintaining high circuit performance. Some of the applications are:

- Radio-frequency transceiver modules for mobile phone handsets (0.9 to 2 GHz)
- Bluetooth\*\* wireless local networking (2.45-5 GHz)

\*Work partially supported by an agency of the U.S. government, not subject to copyright in the U.S.

- Global Positioning System (GPS), with potential installation in mobile hand-sets (1.6 GHz)
- Multi-point multichannel distribution Systems (5.8 GHz and 26-29 GHz)
- Next-generation transmitter/receiver modules for satellite communications (22-24 GHz)
- Advanced automotive control (77 GHz).
- Advanced radio sets (100-300 GHz)

Knowledge of the dielectric constants and loss tangents of LTCC materials at microwave and millimeter wave frequencies is important for design of microwave circuits. These material parameters are needed to obtain the correct characteristic impedance at interconnections and to determine propagation delays and circuit line loss. In general, the LTCC real relative permittivity  $\epsilon'_r$  and the dielectric loss tangent  $\tan \delta$  are functions of frequency and temperature, and should be characterized over the applicable frequency and temperature ranges. Often, the variation of the real permittivity is small in the operational frequency range, but  $\tan \delta$  changes significantly with frequency and should be accurately characterized. In addition, temperature stability of resonant structures fabricated with LTCC materials is essential for good circuit performance. Therefore the temperature coefficient with respect to resonant frequency  $\tau_f$  should be determined over the operational temperature range. LTCC materials with small temperature coefficients are preferred. Other important parameters for circuit design and performance are the surface resistance of the metal used in microstrip lines, accurate control of line geometry to control impedance, and low thickness tolerances for the LTCC layers. Conductors can be directly printed or photo-processed on buried LTCC tapes, allowing for fabrication of multilayered structures of precise-geometry with high conductivity, low-cost conductors. Combined with LTCC tapes that have relatively low dielectric losses, very high-performance, low-cost microwave modules can be fabricated.

Many techniques exist for characterizing dielectric materials. The various techniques differ in the applicable frequency range, accuracy, suitability for variable temperature measurements and sample geometry and preparation [2]. In addition, there are also differences in equipment requirements and in the complexity of data computations. We highlight here the use of microstrip ring resonators, complemented by other resonant measurement techniques, that can be used for the characterization of LTCC material systems at microwave frequencies.

\*\* Certain commercial protocol standards and materials are identified in order to adequately specify the experiments and applications; recommendation or endorsement by NIST is not therein implied.

## RF CHARACTERIZATION OF LTCC MATERIAL SYSTEMS

The most general description of a dielectric material is given by

$$\epsilon^*(f, T) = \epsilon_0 [\epsilon'_r(f, T) - j\epsilon''_r(f, T)] = \epsilon_0 \epsilon'_r(f, T) [1 - j \tan \delta(f, T)], \quad (1)$$

where  $\epsilon_0$  is the permittivity of vacuum ( $8.854 \times 10^{-12}$  F/m),  $\epsilon'_r$  is the real relative permittivity,  $\epsilon''_r$  is the relative loss index,  $\tan \delta$  is the loss tangent,  $f$  is frequency, and  $T$  is temperature. Inhomogeneous dielectrics occur when there are several dielectrics (e.g., air and substrate in microstrip line) or when  $\epsilon'_r$  varies with position in the dielectric. For structures with mixed dielectrics, an *effective permittivity*  $\epsilon'_{r,eff}$  is commonly defined as the ratio of the structure's actual capacitance to the capacitance when the dielectric is replaced by air or vacuum,

$$\epsilon'_{r,eff} = \frac{C_{actual}}{C_{air}}. \quad (2)$$

This definition allows us to treat electromagnetic signal propagation in the structure as propagation in an equivalent or *quasi-TEM* line.

A conventional method used to determine the effective permittivity of a LTCC ceramic and the *overall* insertion loss of the LTCC ceramic and conductor system is the microstrip ring resonator test structure illustrated in Fig. 1. In this test structure, both the ceramic and the microstrip conductor contribute to the total loss. For a low-loss dielectric system, the loss from the conductors is the primary contribution to the total insertion loss  $\alpha_t$  (dB/m) at microwave frequencies. The effective permittivity is the overall effect of the dielectric and the air above the strip lines. Typically, there is a transition from the strip lines to coaxial transmission line cables connected to an automatic network analyzer (ANA). An impedance of 50 ohms is needed for this transition, and the impedance is determined by the width of the strip line and thickness of the dielectric. At resonance and for  $D \gg w$ ,  $\pi D = n\lambda_g$ , where  $D$  is the diameter of the ring resonator,  $w$  is the width of the microstrip,  $\lambda_g = \lambda_0 / \sqrt{\epsilon'_{r,eff}}$  is the guide wavelength,  $\lambda_0$  is the free space wavelength, and  $n = 1, 2, \dots$ . Hence, there are many quasi-transverse electromagnetic (TEM) resonances, given by

$$f = \frac{nc}{\pi D \sqrt{\epsilon'_{r,eff}}}, \quad (3)$$

where  $c$  is the speed of light in free space. An example of the resonance responses is shown in Fig. 2. The frequencies of the resonant peaks can be used to determine the effective real relative permittivity from eq (3), while the resonant frequency, normalized by its 3 dB bandwidth (system  $Q$ -factor), gives information on the overall insertion loss. The overall insertion loss is due to dielectric loss of the LTCC

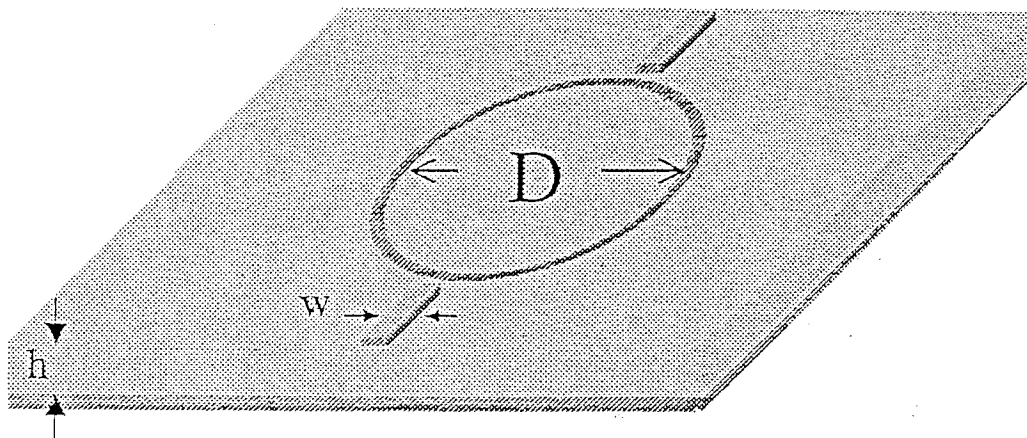


Figure 1: Capacitively coupled ring-resonator test structure on LTCC ceramic with underlying metal ground plane. Diameter of ring resonator is  $D$ , width of microstrip is  $w$  and metal thickness is  $t$ . Thickness of LTCC is  $h$ .

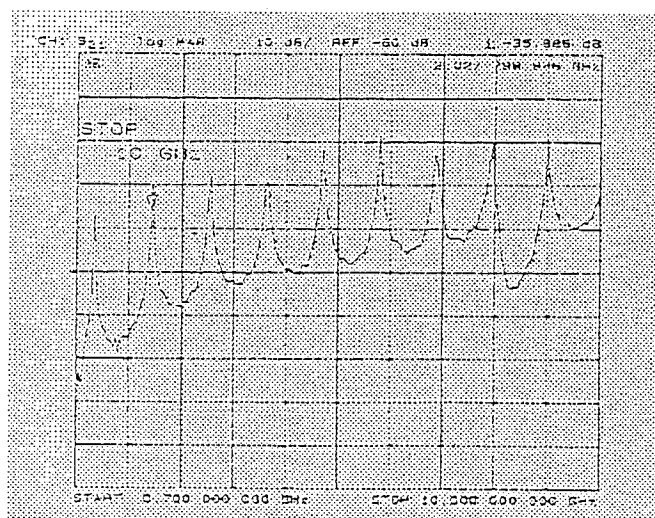


Figure 2: Typical ring resonator transmission response, as measured using the magnitude of the  $S_{21}$  scattering parameter on an ANA.

substrate, and conductive and radiative losses arising from the ring resonator. Ring resonators thus provide a simple and relatively accurate means for measuring the high-frequency effective permittivity and the *total* insertion loss characteristics of LTCC packages that depend on the type of ceramic and processing conditions, conductor metallurgy and surface (pattern) roughness of the conductor. Generally, impedance matching is attained by adjusting the ring's width for a given substrate permittivity and thickness. The circumference of the patterned ring is usually much greater than  $w$  to minimize curvature effects and other parasitics, and the loading effects of the coupling gap on the resonant ring  $Q$ -factor can be accounted for.

The system attenuative properties  $\alpha_t$  as a function of both frequency and temperature  $T$  are the sum of:

- Dielectric loss  $\alpha_d$ ,
- Conductor losses  $\alpha_c$  (consisting of both pattern metal loss  $\alpha_{met}$  and pattern roughness loss  $\alpha_{roughness}$ ),
- Radiation loss  $\alpha_r$  for the microstrip resonator employed.

Hence,

$$\begin{aligned}\alpha_t &= \alpha_d + \alpha_c + \alpha_r \\ &= \alpha_d + \alpha_{met} + \alpha_{roughness} + \alpha_r.\end{aligned}\tag{4}$$

All of the above sources of loss have differing frequency and temperature dependence. In order to define the individual sources of attenuation loss, other measurement methods must be employed to accurately evaluate the intrinsic dielectric properties of the LTCC and the microstrip conductor surface resistance. Only with the use of complementary techniques can we separate the contributions of each loss source to the total insertion loss in LTCC packages at applicable frequencies.

### LTCC Dielectric Property Measurements

Methods for accurately measuring the dielectric properties of LTCC materials may be categorized as:

- Low-frequency capacitor techniques, where use of metallized specimen mitigates depolarization effects, but data results are typically not the same as those at operational RF frequencies,
- Cavity resonator techniques (either closed cylindrical, possibly mode-filtered, and rectangular cavities or open cavities, such as Fabry-Pérot semi-confocal or confocal cavities), and

- Dielectric resonator techniques.

These various dielectric measurement methods are widely reported in the literature, and reviews of applicability and uncertainty analyses are given in [3-5]. Generally, the real permittivity and dielectric loss tangent are determined from measured differences in resonant frequency and  $Q$ -factor, with and without sample insertion. Many dielectric resonator techniques have been developed and include the classical Hakki-Coleman (Courtney) [6,7], the modified Hakki-Coleman [8,9], the Kent dielectrometer (split- cylinder), the coupled split-dielectric resonator, and the sleeve resonator methods [10]. In the Hakki-Coleman method, a cylindrical specimen is used whose aspect ratio and real permittivity determine the resonant frequency. Generally, the dominant, easily identified, low-order  $TE_{011}$  mode is used to determine complex permittivity. In the modified Hakki-Coleman technique, a tunable gap is introduced between the sample under test and the upper ground plane. This allows for measurements of a single specimen's dielectric properties over a tunable frequency range, but the ensuing numerical analysis of the measurement data is more complex. The Hakki-Coleman and modified Hakki-Coleman systems are shown schematically in Fig. 3. Both the Kent dielectrometer [11] and coupled split-post dielectric resonator systems [12,13], also operated in the  $TE_{01}$  mode, permit accurate microwave dielectric measurements of thin, unmetallized laminar substrate specimens. Due to the azimuthal electric-field structure of the  $TE_{01}$  mode, complex permittivity can be measured only in the plane of the specimen (parallel to the ground planes). A schematic of the coupled split-post dielectric resonator system is given in Fig. 4. Both the split-cylinder and the coupled split-post dielectric resonator system are nondestructive and noncontacting, and can be used for rapid checking of dielectric inhomogeneity (permittivity or loss) in the specimen.

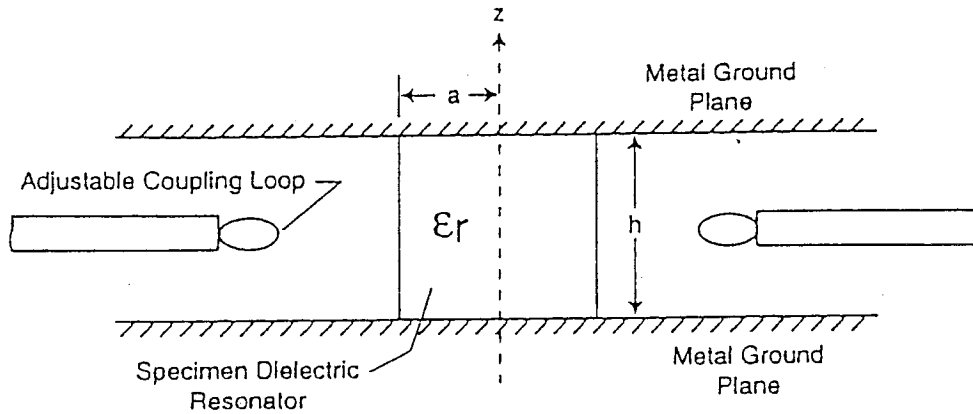
The nominal microwave measurement frequency in the split-post dielectric resonator system is determined by the geometry and permittivity of the coupled low-loss resonators. An upper bound for the systematic or Type B [14] uncertainty in permittivity determination is approximately twice the uncertainty in specimen thickness. Typical absolute measurement uncertainty in dielectric loss tangent is  $2 \times 10^{-5}$ .

### Microstrip Conductor Surface Resistance

The evaluation of attenuative power loss from metallization  $\alpha_{met}$  requires accurate measurements of the surface resistance. Metallization must be thicker than a plane-wave skin depth at the measurement frequency. Either of two dielectric resonator methods can be employed to measure the surface resistance.

In the first method, the metallized specimen is used as a substitution end plate of an ultra-low loss, c-axis oriented, single-crystal sapphire or single-crystal quartz di-

## CLASSICAL COURTNEY MEASUREMENT



## MODIFIED COURTNEY MEASUREMENT

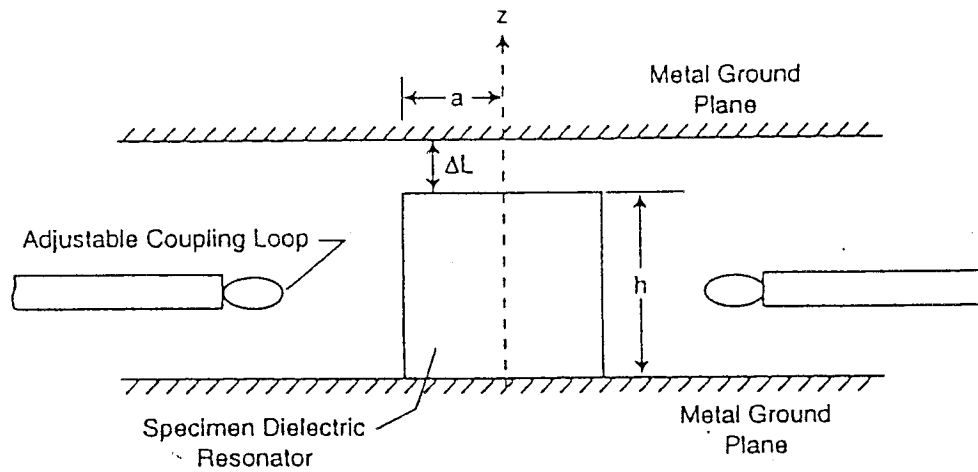


Figure 3: Classical and modified Hakki-Coleman (Courtney) systems for microwave dielectric measurements.

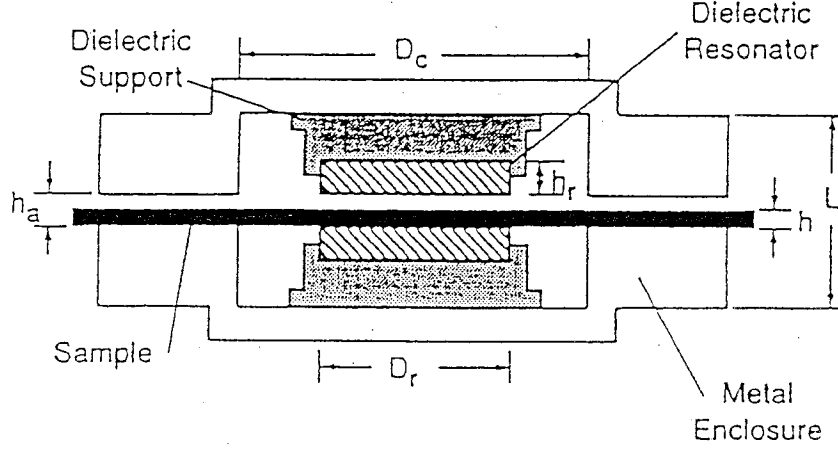


Figure 4: Coupled split-post dielectric resonator system.

electric resonator in the Courtney configuration. The surface resistance of the metal ground planes  $R_{s,gp}$  of the Courtney system is first determined from the unloaded  $Q$ -factor,  $Q_{c1}$ , and the  $TE_{011}$  resonant frequency data. The resonant frequency is determined by the aspect ratio of the ultra-low loss oriented single crystal and its permittivity normal to the  $c$ -axis. The unloaded  $Q$ -factor  $Q_{c2}$  with the metallized specimen as a substitution endplate is then measured in this configuration. The specimen surface resistance  $R_{s,spec}$  is given by

$$R_{s,spec} = \left[ 2 \frac{Q_{c1}}{Q_{c2}} - 1 \right] R_{s,gp}, \quad (5)$$

from which we can compute the conductivity  $\sigma = \pi f \mu_0 / R_{s,spec}^2$ , where  $\mu_0$  is the free space permeability ( $4\pi \times 10^{-7} \text{H/m}$ ).

In the second method, combinations of three metallized specimens are used as the end plates of an ultra-low loss,  $c$ -axis oriented, single-crystal sapphire or single-crystal quartz dielectric resonator in the Courtney configuration. In this case, the specimen surface resistance is given by

$$R_{s,spec} = A \left( Q_0^{-1} - p_e \tan \delta \right), \quad (6)$$

where  $Q_0$  is the measured unloaded  $Q$ -factor,  $p_e$  is the dielectric resonator electric energy filling factor, and  $A$  is a geometric factor. The filling factor and geometric

factor are given by

$$p_e = 1 / \left[ 1 + \frac{1}{\epsilon'_{r,crys}} F(x_{01}) G(y_{01}) \right], \quad (7)$$

and

$$A = \frac{2\pi f^3 \mu_0^2 \epsilon_0 h^3 [\epsilon'_{r,crys} + F(x_{01}) G(y_{01})]}{1 + F(x_{01}) G(y_{01})}, \quad (8)$$

where

$$F(x_{01}) = \frac{J_1^2(x_{01})}{J_1^2(x_{01}) - J_0(x_{01}) J_2(x_{01})}, \quad (9)$$

$$G(y_{01}) = \frac{K_0(y_{01}) K_2(y_{01}) - K_1^2(y_{01})}{K_1^2(y_{01})}, \quad (10)$$

$$y_{01} = \sqrt{(k_0 a)^2 (\epsilon'_{r,crys} - 1) - x_{01}^2}, \quad (11)$$

and

$$k_0^2 = 4\pi^2 f^2 \mu_0 \epsilon_0. \quad (12)$$

In (9-11),  $\epsilon'_{r,crys}$  is the real relative permittivity of the crystal dielectric resonator normal to the c-axis, and  $J_1, J_2$  and  $K_0, K_2$  are Bessel functions and modified Bessel functions. The parameters  $x_{01}$  and  $y_{01}$  are determined from the first eigenvalue permittivity root of the equation

$$\frac{J_1(x_{01})}{x_{01}} + \frac{K_1(y_{01}) J_0(x_{01})}{y_{01} K_0(y_{01})} = 0, \quad (13)$$

plus the resonant condition  $(k_0 a)^2 = (a\pi/h)^2 + x_{01}^2$ , given the TE<sub>011</sub> resonant frequency, and the radius and height of the crystal dielectric resonator [15]. Typical room temperature total uncertainty for surface resistance measurements is  $\pm 0.1$  m $\Omega$ .

Once the surface resistance is determined, its value at other frequencies can be scaled according to the square root of frequency for normal metal conductors. Attenuative losses for microstrip metal conductors can then be computed.

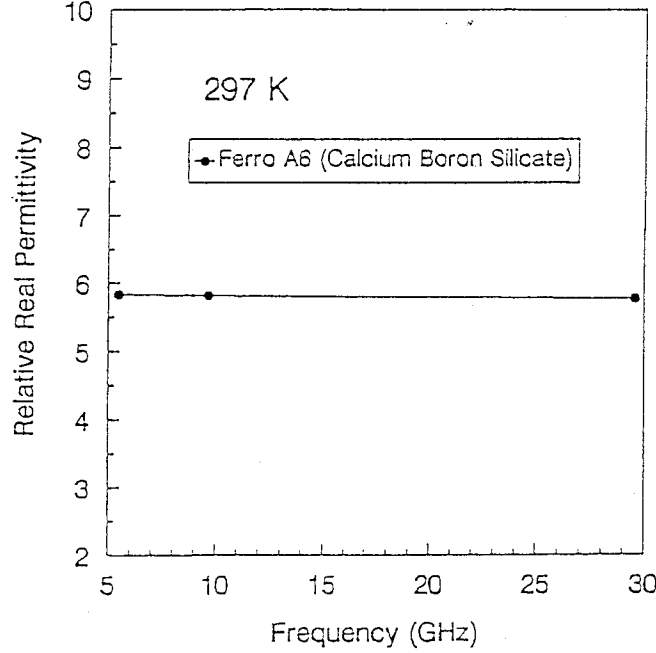


Figure 5: Relative real permittivity of calcium boron silicate (A6) LTCC substrates. Total estimated measurement uncertainty is 0.5%.

## COMPARISON OF RING RESONATOR MEASUREMENTS TO THEORETICAL PREDICTIONS

Measured permittivities and dielectric loss tangents for laminar A6 LTCC specimens (calcium boron silicates) are shown as a function of frequency in Figs. 5 and 6. These measurements were performed with three split-post dielectric resonator systems, for which the uncertainties in real permittivity and dielectric loss tangent are 0.5% and  $2 \times 10^{-5}$ . Surface resistance of the silver conductor used with the A6 LTCC was measured at 297 K with c-axis oriented single-crystal sapphire dimensioned for  $TE_{011}$  resonance at 10 GHz. The three-sample method was employed at 10 GHz; the scaled surface resistance values from 5-35 GHz are shown in Fig. 7. The average measured surface resistance at 10 GHz and 297 K is  $29 \pm 0.1$  m $\Omega$ , which gives an average conductivity of  $4.65 \times 10^7$  S/m.

Total attenuative insertion losses, as measured with a microstrip ring resonator having  $w=0.9144$  mm,  $h=0.6096$  mm ( $w/h=1.5$ ), and  $D=43.18$  mm, are shown in Fig. 8. Metallization thickness varies between 5 and 8  $\mu$ m, which is much thicker than the plane-wave skin depth  $\delta = 1/\sqrt{2\pi f \mu_0 \sigma}$  of 0.5  $\mu$ m at 10 GHz. The metallization used a silver conductor system, developed to minimize conductor losses, in contrast to traditional Ag/Pd and Ag/Pt. The pure silver metallurgy reduces cost, improves microwave performance, and offers improved solder leach

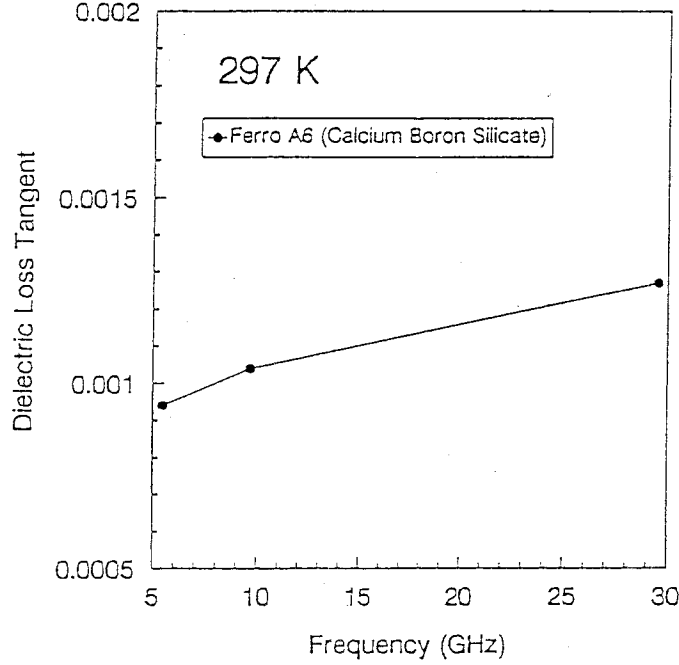


Figure 6: Dielectric loss tangent of calcium boron silicate (A6) LTCC substrates. Estimated systematic (Type B) measurement uncertainty is  $2 \times 10^{-5}$ .

resistance [16].

### Dielectric Attenuative Insertion Loss

The *effective* dielectric loss in microstrip transmission lines is an important parameter used in designing hybrid integrated circuits that require small attenuation. This loss can be calculated *if* the loss tangent of the dielectric substrate and the electric field distribution inside the substrate are known. Electric field computations are usually complicated and not practical for design purposes. Hence, we need a simple and accurate method for calculating the dielectric attenuation loss from other well-known properties of the microstrip transmission line. Schneider et al. [17,18] have derived general design equations valid for all microstrip transmission lines provided that the propagating mode can be approximated by a quasi-TEM mode. In this case, the dielectric attenuation loss is

$$\begin{aligned}
 \alpha_d &= \frac{20\pi}{\ln(10)} \frac{q \tan \delta}{\lambda_g} \\
 &= \frac{27.3}{\lambda_g} \tan \delta_{eff},
 \end{aligned} \tag{14}$$

where  $q$  is the filling factor of a microstrip, which is the ratio of electric field energy

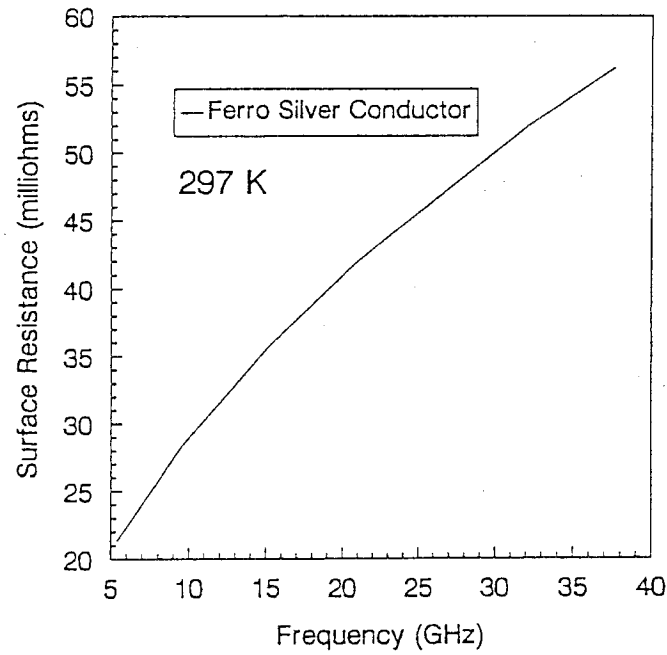


Figure 7: Surface resistance of Ag conductor on A6 LTCC substrate as a function of frequency.

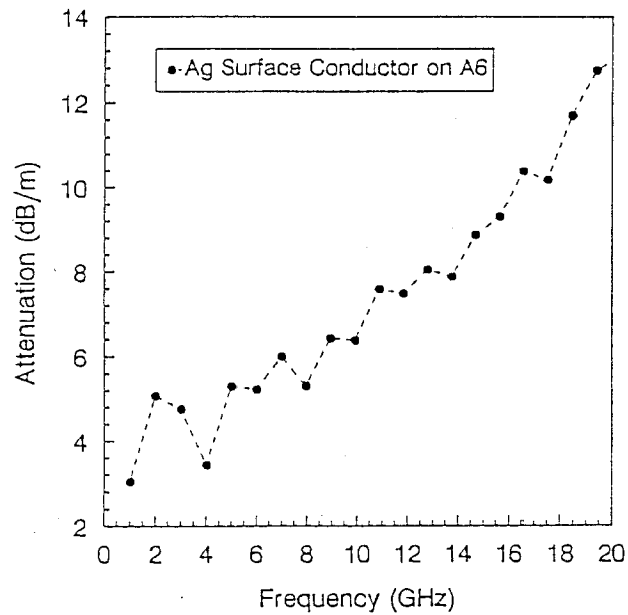


Figure 8: Total insertion losses measured with microstrip ring resonator test fixture.

stored in the dielectric to the total electric field energy of the microstrip, given by

$$q = \frac{\epsilon'_{r,eff}\epsilon'_r - \epsilon'_r}{\epsilon'_{r,eff}\epsilon'_r - \epsilon'_{r,eff}}. \quad (15)$$

In (14),  $\tan \delta_{eff}$  is the *effective* dielectric loss tangent given by the product of the filling factor and the intrinsic substrate dielectric loss tangent,

$$\tan \delta_{eff} = q \tan \delta, \quad (16)$$

and  $\lambda_g$  is the guide wavelength previously defined. The effective dielectric constant for the standard microstrip is approximated by Schneider [19] as

$$\epsilon'_{r,eff} = \frac{\epsilon'_r + 1}{2} + \frac{\epsilon'_r - 1}{2} \left(1 + \frac{10h}{w}\right)^{-\frac{1}{2}}. \quad (17)$$

Note that the effective relative permittivity,  $\epsilon'_{r,eff}$ , is not the same parameter as the intrinsic relative permittivity,  $\epsilon'_r$ , of the substrate; the two parameters cannot be compared directly. Schneider's relation for  $\epsilon'_{r,eff}$  has been improved by Hammerstad and Bekkadal [20], depending on whether  $w/h \leq 1$  or  $w/h \geq 1$ :

$$\epsilon'_{r,eff} = \frac{\epsilon'_r + 1}{2} + \frac{\epsilon'_r - 1}{2} \left[ \left(1 + \frac{12h}{w}\right)^{-\frac{1}{2}} + 0.04 \left(1 - \frac{w}{h}\right)^2 \right], \quad w/h \leq 1, \quad (18)$$

and

$$\epsilon'_{r,eff} = \frac{\epsilon'_r + 1}{2} + \frac{\epsilon'_r - 1}{2} \left[1 + \frac{12h}{w}\right]^{-\frac{1}{2}}, \quad w/h \geq 1. \quad (19)$$

The latter two equations for the  $\epsilon'_{r,eff}$  are accurate to within 1% for  $\epsilon'_r \leq 16$  and for  $0.05 \leq w/h \leq 20$ . For  $\epsilon'_r > 16$  or for  $w/h < 0.05$ , the error is less than 2 %.

Effective permittivity data obtained from the microstrip ring resonator measurements using eq (3) are shown in Fig. 9. The effective permittivities calculated from the LTCC substrate dielectric measurement data given in Fig. 5 using eq (19) closely agree with the effective permittivity data of Fig. 9. At 10 GHz and 297 K,  $\epsilon'_{r,eff} = 4.30$ ,  $q = 0.67$ , and  $\tan \delta_{eff} = 6.9 \times 10^{-4}$ . Hence, at this frequency and temperature, the theoretical attenuation loss from the dielectric LTCC substrate would be 2.69 dB/m. Similar computations can be performed at other frequencies.

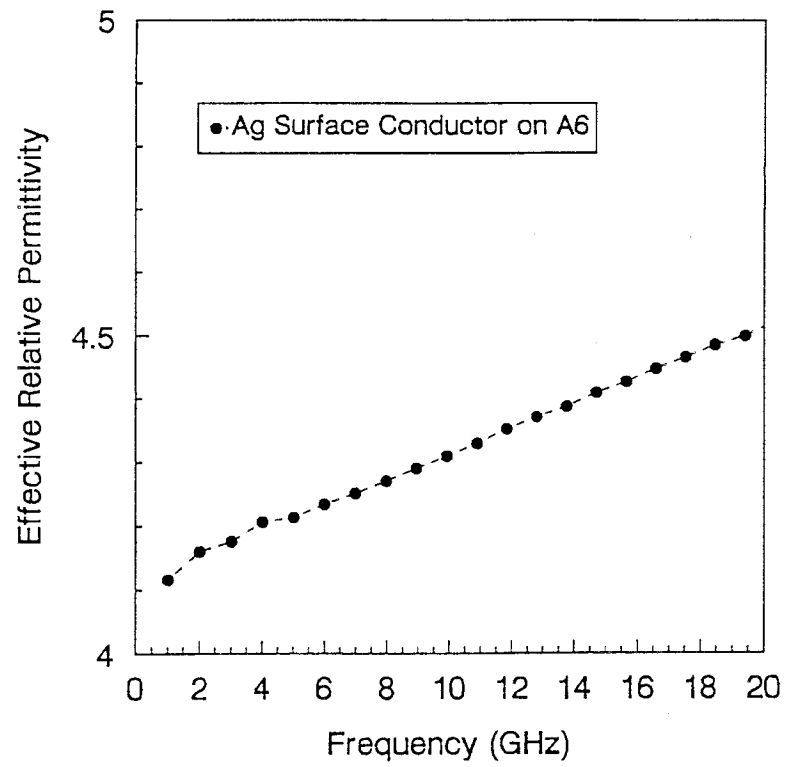


Figure 9: Effective relative dielectric constant on (A6) calcium boron silicate as function of frequency, determined from microstrip ring resonator measurements.

## Metal Insertion Loss

Conductor losses from the microstrip ring resonator test coupon result from several contributing factors. These are the actual conductivity of the patterned metal material and the frequency-dependent skin effects. Depending on  $R_s$ ,  $w/h$ , and  $f$ , the effects of the ground plane on conductor losses must also be taken into account. In addition, there are pattern roughness loss effects, which should be treated separately. For perfectly smooth microstrip ring conductors, Schneider et al. [17] give the following relations for conductor losses due only to skin effect and metal surface resistance,

$$\alpha_{met} = \frac{10R_s}{\pi \ln 10} \frac{\left[\frac{8h}{w} - \frac{w}{4h}\right] \left[1 + \frac{h}{w} + \frac{h}{w} \frac{\partial w}{\partial t}\right]}{hZ_0 e^{Z_0/60}}, \quad w/h \leq 1 \quad (20)$$

and

$$\alpha_{met} = \frac{Z_0 R_s}{720\pi^2 h \ln 10} \left[ 1 + \frac{0.44h^2}{w^2} + \frac{6h^2}{w^2} \left(1 - \frac{h}{w}\right)^5 \right] \cdot \left(1 + \frac{w}{h} + \frac{\partial w}{\partial t}\right), \quad w/h \geq 1, \quad (21)$$

where  $Z_0$  is the characteristic impedance of the ring resonator (here 50 ohms) and

$$\frac{\partial w}{\partial t} = \frac{1}{\pi} \ln \frac{4\pi w}{t}, \quad \frac{w}{h} \leq \frac{1}{2\pi}, \quad (22)$$

or

$$\frac{\partial w}{\partial t} = \frac{1}{\pi} \ln \frac{2h}{t}, \quad \frac{w}{h} \geq \frac{1}{2\pi}. \quad (23)$$

The above equations are valid when the microstrip and ground plane conductivities are the same and for  $t \ll h/2$  and  $\partial w/\partial t > 1$ . Purcel, Masse, and Hartwig [21] have also given similar equations for evaluation of the attenuation constant of planar microstrip transmission lines, using Wheeler's incremental inductance rule [22]. These rules generally work well provided that the ratio  $t/\delta \gg 1$ . However, when the thickness  $t$  is comparable to or less than the skin depth, or when the fabricated strip conductors are not exactly rectangular in cross-section, but are instead trapezoidal, these rules often give poor results. For these cases, Holloway and Kuester [23,24] and Holloway [25] have developed quasi-closed form expressions for the integral expression:

$$\begin{aligned} \alpha_{met} &\approx \frac{R_s}{2Z_0} \int_{top+bot} \left(\frac{J_s}{I}\right)^2 dl, \\ &\approx \frac{R_{sm}}{2Z_0\pi^2} \frac{\ln\left(\frac{w}{\Delta} - 1\right)}{w}, \end{aligned} \quad (24)$$

where

$$R_{sm} = 2\pi f\mu_0 t \operatorname{Im} \left( \frac{\cot(k_c t) + \csc(k_c t)}{k_c t} \right), \quad (25)$$

$k_c$  is the complex wavenumber in the conductor,  $\operatorname{Im}$  denotes the imaginary part, and  $\Delta$  is a numerically determined *stopping* distance parameter for the line integral evaluation that depends on the local microstrip edge geometry (shape of edge and electrical thickness).

In any of the above relations for the conductor attenuation loss of the microstrip ring resonator, the intrinsic metal surface resistance  $R_s$  is required. In Fig. 10 the quasi-closed expressions from Holloway and Kuester were used to compute the metal conductor losses of the microstrip ring resonator as a function of frequency. At 10 GHz and 297 K, the calculated metal loss attenuation from a perfectly smooth microstrip ring resonator having a conductivity of  $4.65 \times 10^7$  S/m, exclusive of ground plane effects, is 2.70 dB/m. For illustration purposes, we have also included the attenuation of a microstrip ring resonator with the same geometric parameters at 10 GHz, using a conductivity of  $6.17 \times 10^7$  for bulk pure silver given by Montgomery, Dicke, and Purcell [27].

As frequency or  $w/h$  increases, attenuative losses from the ground plane more strongly influence microstrip ring resonator data. The dependence on frequency results from an increased surface resistance  $R_s$  of the metal used in stripline patterning as frequency increases. Holloway and Hufford have separately treated the conductor loss associated with the ground plane of a microstrip line [28]. With the assumption that the actual current density on the surface of a highly conducting ground plane is perturbed only slightly from that of a perfect conductor, the following expression was derived for ground plane attenuation  $\alpha_{gr}$ :

$$\alpha_{gr} = \frac{R_s}{Z_0 w \pi} \left( \tan^{-1} \left( \frac{w}{2h} \right) - \frac{h}{w} \ln \left[ 1 + \left( \frac{w}{2h} \right)^2 \right] \right). \quad (26)$$

At 10 GHz, the surface resistance for the Ag metal system reported here is 29 milliohm,  $Z_0=50$  ohm, and  $w/h = 1.5$ , so that the ground plane contribution to the microstrip ring resonator measurements is 0.067 dB/m.

Two remaining frequency-dependent effects for the microstrip ring resonator technique used in characterization of LTCC material systems must be considered. First, in any resonant system that might be employed for accurate microwave dielectric or metal surface resistance measurements, radiation losses, especially if unavoidable, must be evaluated. Second, the effects of metal pattern roughness must be considered.

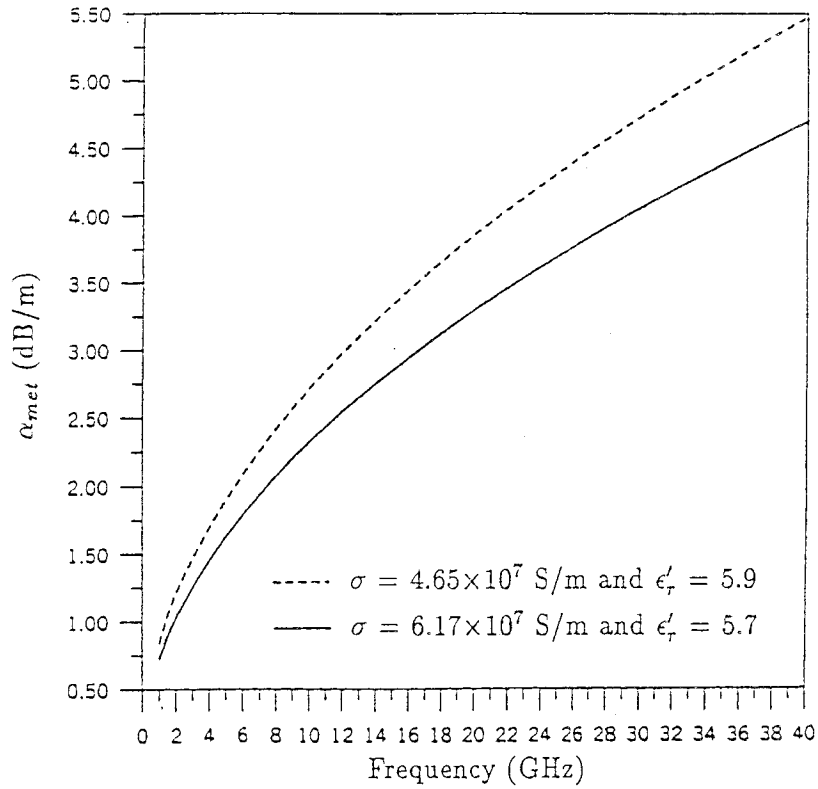
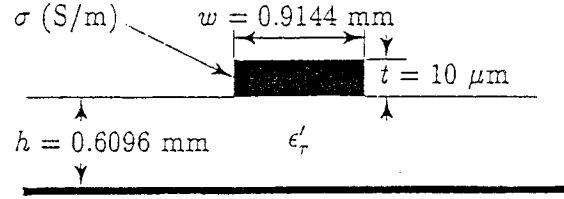


Figure 10: Conductor attenuation loss for microstrip ring resonator, exclusive of ground plane effects, conductor roughness and radiation (after Holloway [26]).

## Radiation Insertion Loss

Radiative losses of various microstrip configurations have been considered [29,30]. With the recognition that the quality factor of a circular resonator is approximately equal to that of a stretched open-ended resonator, the following relation for radiation loss from an impedance-matched microstrip line was derived [30]:

$$\alpha_r = 60 \left( \frac{2\pi h}{\lambda_0} \right)^2 F(\epsilon'_{r,eff}), \quad (27)$$

where

$$F(\epsilon'_{r,eff}) = 1 - \frac{\epsilon'_{r,eff} - 1}{2\sqrt{\epsilon'_{r,eff}}} \log \left( \frac{\sqrt{\epsilon'_{r,eff} + 1}}{\sqrt{\epsilon'_{r,eff} - 1}} \right). \quad (28)$$

With the ring resonator system employed, we calculated a radiative loss of approximately 0.5 dB/m at 10 GHz.

## Effect of Conductor Surface Roughness

In all the above formulas the conductor surface is assumed to be perfectly smooth. However, the fabrication processes create scratches and random bumps in real-world conductors. An example of conductor surface roughness for the LTCC system reported here is illustrated in Fig. 11.

Generally, as frequency increases, the surface roughness of the conductor in the LTCC system becomes large relative to a skin depth, and surface roughness effects contribute more to attenuation losses. This is discussed in detail by Sanderson [31], where the following approximate relation is given for conductor losses due to surface roughness in terms of the metal loss calculated for a perfectly smooth conductor  $\alpha_{met}$ , the rms surface roughness  $\Lambda$ , and the electrical skin depth  $\delta$ :

$$\alpha_{roughness} = \alpha_{met} \left[ 1 + \frac{2}{\pi} \tan^{-1} \left[ 1.4 \left( \frac{\Lambda}{\delta} \right)^2 \right] \right]. \quad (29)$$

At 10 GHz, the loss due to metal roughness illustrated in Fig. 11 is estimated to be 0.17 dB/m. A comparison of the separately calculated insertion losses of the dielectric LTCC substrate and fabricated metal with observed resonant frequency and total insertion loss data can now be made. The individually contributing effects of insertion loss for both the LTCC dielectric and metal require auxiliary methods that accurately characterize the intrinsic dielectric properties of the LTCC substrate and the surface resistance of the metal used in patterning circuits. At 10 GHz,

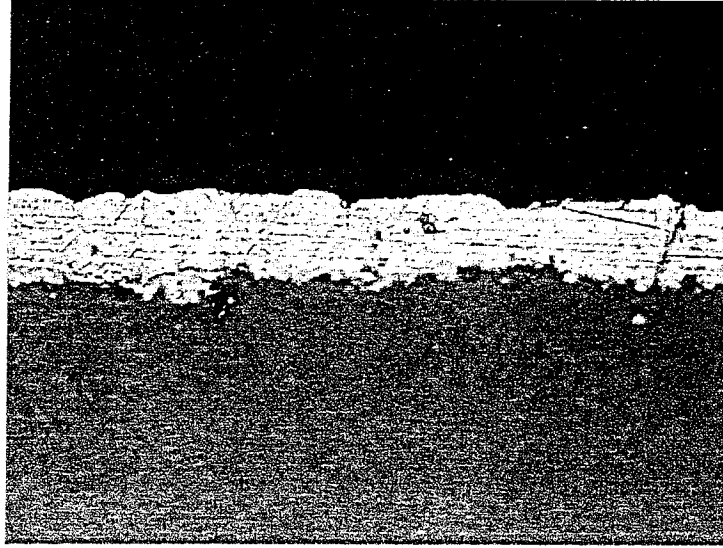


Figure 11: Typical surface roughness of Ag silver metallization on A6 LTCC substrate. RMS conductor thickness is  $10\text{ }\mu\text{m}$ , and average surface roughness is  $1.4\text{ }\mu\text{m}$ . Horizontal scale is same as vertical scale.

the total calculated insertion losses for the system reported were  $\alpha_{t,calc} = \alpha_d + \alpha_{met} + \alpha_{roughness} + \alpha_r = 6.13\text{ dB/m}$ . From Fig. 8, the measured microstrip ring resonator total attenuation insertion loss,  $\alpha_{t,meas}$ , is  $6.37\text{ dB/m}$  at  $10\text{ GHz}$ , yielding a difference of  $+0.24\text{ dB/m}$  ( $+5.3\%$ ) between measured data for total insertion loss of a microstrip ring resonator and insertion loss calculated from the intrinsic properties of the LTCC and metal used in patterning. Similar comparisons can be performed at other resonant frequencies.

## SUMMARY

The microwave properties of LTCC material systems need to be accurately evaluated and related to intrinsic substrate dielectric and conductor metallurgy, as well as processing and fabrication conditions. A microstrip ring resonator with suitable dimensions patterned on the LTCC substrate can be employed for quantifying *total* insertion loss effects of the LTCC dielectric and the metal system used in circuit patterning, as well as practical pattern fabrication issues. Separate identification of each source of attenuation loss *requires* auxiliary techniques that accurately determine the intrinsic dielectric properties of the substrate and the surface resistance of the metal used in patterning. Accurate analytical expressions for evaluating criti-

cal microwave performance parameters, together with their limitations, have been presented that are valid for any LTCC material system.

## ACKNOWLEDGMENTS

The authors acknowledge Chris Holloway, Michael Janezic and Jim Baker-Jarvis for useful discussions, and thank Chris Holloway for calculations of conductor attenuation.

## REFERENCES

- <sup>1</sup>P. Barnwell, W. Zhang, and T. Hochheimer, "LTCC Systems for Low GHz Frequencies-the Critical Properties," *Proc. IMAPS Advanced Technology Workshop on Ceramic Technologies for Microwave: Handsets; Bluetooth; Broadband; LMDS*, March 26-27, Denver, CO (2001).
- <sup>2</sup>J. Baker-Jarvis, M.D. Janezic, B. Riddle, C.L. Holloway, N.G. Paulter, J.E. Blendell, "Dielectric and Conductor-Loss Characterization and Measurements on Electronic Packaging Materials," *Nat'l. Inst. Stand. Techn. Tech. Note 1520*, 2001.
- <sup>3</sup>R.G. Geyer and J. Krupka, "Microwave Dielectric Property Measurements," in *Dielectric Materials and Devices, Proc. Am. Cer. Soc.*, 533-560 (2002).
- <sup>4</sup>J. Krupka and R.G. Geyer, "Loss-Angle Measurements," in J.G. Webster, ed., *Encyclopedia of Elec. and Electron. Eng.*, John Wiley, New York (1999).
- <sup>5</sup>J. Baker-Jarvis, R.G. Geyer, J.H. Grosvenor, Jr., M.D. Janezic, C.A. Jones, B. Riddle, and C.M. Weil, "Dielectric Characterization of Low Loss Materials: a Comparison of Techniques," *IEEE Trans. on Dielectrics and Electrical Insulation*, **5** 571-577 (1998)
- <sup>6</sup>B.W. Hakki and P.D. Coleman, "A Dielectric Resonator Method of Measuring Inductive Capacities in the Millimeter Range," *IEEE Trans. Microwave Theory Tech.*, **MTT-8** 402-410 (1960).
- <sup>7</sup>W.E. Courtney, "Analysis and Evaluation of a Method of Measuring the Complex Permittivity and Permeability of Microwave Insulators," *IEEE Trans. Microwave Theory Tech.*, **MTT-18** 476-485 (1970)
- <sup>8</sup>Y. Kobayashi, T. Aoki, and Y. Kabe, "Influence of Conductor Shields on the Q-Factors of a TE<sub>0</sub> Dielectric Resonator," *IEEE MTT-S Int. Microwave Symp.*

*Digest, St. Louis*, 281-284 (1985).

<sup>9</sup> J. Krupka, R.G. Geyer, and D. Cros, "Measurements of Permittivity and the Dielectric Loss Tangent of Low Loss Dielectric Materials with a Dielectric Resonator Operating on the Higher Order  $TE_{0\gamma\delta}$  Modes," *MIKON X Int. Microwave Conf. Proc.*, Vol. 2, 567-572 (1994).

<sup>10</sup> R.G. Geyer, P. Kabos, and J. Baker-Jarvis, "Dielectric Sleeve Resonator Techniques for Microwave Complex Permittivity Evaluation," *IEEE Trans. Instr. Meas.*, **51** 1-10 (2002).

<sup>11</sup> G. Kent, "An Evanescent-Mode Tester for Ceramic dielectric Substrates," *IEEE Trans. Microwave Theory Tech.*, **36** 1451-1454 (1988).

<sup>12</sup> J. Krupka, R.G. Geyer, J. Baker-Jarvis, and J. Ceremuga, "Measurements of the Complex permittivity of Microwave Circuit Board Substrates Using Split Dielectric Resonator and Reentrant Cavity Techniques," in *DMMA'96 Conf. Proc.*, Bath, U.K., 21-24 (1996).

<sup>13</sup> J. Krupka, A.P. Gregory, O.C. Rochard, R.N. Clarke, B. Riddle, and J. Baker-Jarvis, "Uncertainty of Complex Permittivity Measurements by Split-Post Dielectric Resonator Technique," *Jour. European Cer. Soc.*, **21** 2673-2676 (2001).

<sup>14</sup> B.N. Taylor and C.E. Kuyatt, "Guidelines for Evaluating and Expressing the Uncertainty of NIST Measurement Results," *NIST Techn. Note 1297*, (1994).

<sup>15</sup> D. Kajfez and P. Guillon, *Dielectric Resonators*, Artech House (1986).

<sup>16</sup> L. Chai, A. Shaikh, and V. Stygar, "New Generation Silver Conductor System for LTCC Applications," *Proc. Wireless Symposium*, February 12-16, San Jose, CA (2001).

<sup>17</sup> M.V. Schneider, B. Glance, and W.F. Bodtmann, "Microwave and Millimeter Wave Hybrid Integrated Circuits for Radio System," *Bell Systems Tech. Jour.*, **48** 1703-1726 (1969).

<sup>18</sup> M.V. Schneider, "Dielectric Loss in Integrated Microwave Circuits," *Bell Systems Tech. Jour.*, **48** 2325-2332 (1969).

- <sup>19</sup>M.V. Schneider, "Microstrip Lines for Microwave Integrated Circuits," *Bell Systems Tech. Jour.*, **48** 1421-1444 (1969).
- <sup>20</sup>E.O. Hammerstad and F. Bekkadal, *Microstrip Handbook*, the University of Trondheim, ELAB Rpt. STF44 A74169 (1975).
- <sup>21</sup>R.A. Purcel, D.J. Masse, and C.P. Hartwig, "Losses in Microstrip," *IEEE Trans. Microwave Theory Tech.*, **12** 342-350 (1968).
- <sup>22</sup>H.A. Wheeler, "Transmission-Line Properties of a Strip on a Dielectric Sheet on a Plane," *IEEE Trans. Microwave Theory Tech.*, **25** 631-647 (1977).
- <sup>23</sup>C.L. Holloway and E.F. Kuester, "Edge Shape Effects and Quasi-Closed Form Expressions for the Conductor Loss of Microstrip Lines," *Radio Science*, 539-559 (1994).
- <sup>24</sup>C.L. Holloway and E.F. Kuester, "A Quasi-Closed Form Expression for the Conductor Loss of CPW Lines, with an Investigation of Edge Shape Effects," *IEEE Trans. Microwave Theory Tech.*, **43** 2695-2701 (1995).
- <sup>25</sup>C.L. Holloway, "Expression for the Conductor Loss of Strip-Line and Coplanar-Strip (CPS) Structures," *Microwave and Optical Technology Letters*, **25** 162-168 (2000).
- <sup>26</sup>C.L. Holloway, personal communication.
- <sup>27</sup> C.G. Montgomery, R.H. Dicke, and E.M. Purcell, Principles of Microwave Circuits, *IEE Electromagnetic Wave Series 25*, Peter Peregrinus, Ltd., U.K. p.47 (1987).
- <sup>28</sup>C.L Holloway and G.A. Hufford, "Internal Inductance and Conductor Loss Associated with the Ground Plane of a Microstrip Line," *IEEE Trans. on Electromagnetic Compatibility*, **39** 73-78 (1997).
- <sup>29</sup>L.J. Van Der Pauw, "The Radiation of Electromagnetic Power by Microstrip Configurations," *IEEE Trans. Microwave Theory Tech.*, **25** 719-725 (1977).
- <sup>30</sup>M.D. Abouzahra and L. Lewin, "Radiation from Microstrip Discontinuities," *IEEE Trans. Microwave Theory Tech.*, **27** 722-723 (1979).

<sup>31</sup>A.E. Sanderson, "Effect of Surface Roughness on Propagation of the TEM Mode," in *Advances in Microwaves*, Leo Young, Ed., Academic Press, New York, **7** 2-57 (1971).